# Verification of Universal Relations in a Strongly Interacting Fermi Gas

J. T. Stewart, J. P. Gaebler,* T. E. Drake, and D. S. Jin†

*JILA, National Institute of Standards and Technology and Department of Physics, University of Colorado, Boulder, Colorado 80309-0440, USA*

(Received 9 February 2010; revised manuscript received 27 April 2010; published 7 June 2010)

Many-body fermion systems are important in many branches of physics, including condensed matter, nuclear, and now cold atom physics. In many cases, the interactions between fermions can be approximated by a contact interaction. A recent theoretical advance in the study of these systems is the derivation of a number of exact universal relations that are predicted to be valid for all interaction strengths, temperatures, and spin compositions. These equations, referred to as the Tan relations, relate a microscopic quantity, namely, the amplitude of the high-momentum tail of the fermion momentum distribution, to the thermodynamics of the many-body system. In this work, we provide experimental verification of the Tan relations in a strongly interacting gas of fermionic atoms by measuring both the microscopic and macroscopic quantities in the same system.

DOI: 10.1103/PhysRevLett.104.235301 PACS numbers: 67.85.Lm, 05.30.Fk, 71.27.+a

In 2005, Shina Tan derived a number of universal relations for an interacting Fermi gas with short-range, or contact, interactions [1]. These powerful relations connect microscopic quantities, such as the momentum distribution of the fermions, to macroscopic quantities, such as the total energy of the system [1,2,4,5]. Furthermore, the relations are universal in that they do not depend on the details of the interparticle potential, nor do they depend on the state of the system, which could be an exotic Fermi superfluid, a normal Fermi liquid, or even a simple two-body state such as a diatomic molecule. At the heart of the universal relations is a single quantity, which Tan termed the contact. The contact is defined as the amplitude of the high-$k$ tail of the momentum distribution $n(k)$, which was previously predicted to scale as $1/k^4$ for an interacting Fermi gas [3]. Remarkably, it can be shown that the contact encapsulates all of the many-body physics [4]. Two recent works derived additional universal relations, which allowed the contact for a strongly interacting Fermi gas to be extracted from measurements of the closed channel fraction [5,6] and inelastic Bragg scattering [7]; these results were in good agreement with theoretical predictions for the BCS-BEC crossover. Here, we present a series of measurements that not only measure the contact in the BCS-BEC crossover with multiple techniques, but moreover test the Tan relations by comparing measurements of both microscopic and macroscopic quantities in the same system. We directly verify the universal relations by exploiting the fact that while the value of the contact depends on the many-body state and on parameters such as temperature, number density, and interaction strength, the universal relations do not.

Our measurements are done in an ultra cold gas of fermionic $^{40}$K atoms confined in a harmonic trapping potential. We cool the gas to quantum degeneracy in a far-detuned optical dipole trap as described in previous work [8]. The trap is axially symmetric and parameterized by a radial trap frequency, which varies for these data from $\omega_r = 2\pi \times 230$ to $2\pi \times 260$ Hz, and an axial trap frequency, which varies from $\omega_z = 2\pi \times 17$ to $2\pi \times 21$ Hz. We obtain a 50/50 mixture of atoms in two spin states, namely, the $|f, m_f\rangle = |9/2, -9/2\rangle$ and $|9/2, -7/2\rangle$ states, where $f$ is the total atomic spin and $m_f$ is the projection along the magnetic-field axis. Our final stage of evaporation occurs at a magnetic field of 203.5 G, where the $s$-wave scattering length, $a$, that characterizes the interactions between atoms in the $|9/2, -9/2\rangle$ and $|9/2, -7/2\rangle$ states is approximately 800 $a_0$, where $a_0$ is the Bohr radius. At the end of the evaporation, we have $10^5$ atoms per spin state at a normalized temperature $\frac{T}{T_F} = 0.11 \pm 0.02$, where the Fermi temperature $T_F$ corresponds to the Fermi energy, $E_F = k_b T_F = \hbar\omega(6N)^{1/3}$. Here, $N$ is the atom number in one spin state, $\omega = (\omega_r^2 \omega_z)^{1/3}$, and $k_b$ is the Boltzmann constant. After the evaporation, we increase the interaction strength adiabatically with a slow magnetic-field sweep to a Fano-Feshbach scattering resonance.

Following Tan [1], we define the integrated contact per particle for the trapped gas from the momentum distribution of the fermions, $n(k)$, using [9]

$$C = \lim_{k\to\infty} k^4 n(k). \tag{1}$$

Here, $k$ is the wave number in units of the Fermi wave number, $k_F = \frac{\sqrt{2mE_F}}{\hbar}$, and $n(k)$ for a 50/50 spin mixture is normalized such that $\int_0^\infty \frac{n(k)}{(2\pi)^3} d^3k = 0.5$. We directly measure $n(k)$ using ballistic expansion of the trapped gas, where we turn off the interactions for the expansion. We accomplish this by rapidly sweeping the magnetic field to 209 G where $a$ vanishes, and then immediately turning off the external trapping potential [10] and taking an absorption image of the cloud after 6 ms of expansion. The probe light for the imaging propagates along the axial direction of the trap, and thus we measure the radial momentum distribution. Assuming the momentum distribution is spherically symmetric, we obtain $n(k)$ with an inverse Abel transform.

Figure 1(a) shows an example $n(k)$ for a strongly interacting gas with a dimensionless interaction strength $(k_F a)^{-1}$ of $-0.08 \pm 0.04$. The measured $n(k)$ exhibits a $1/k^4$ tail at large $k$, and we extract $C$ from the average value of $k^4 n(k)$ for $k > k_C$, where we use $k_C = 1.85$ for $(k_F a)^{-1} > -0.5$ and $k_C = 1.55$ for $(k_F a)^{-1} < -0.5$. These values for $k_C$ are chosen empirically such that for $k \geq k_C$, the momentum distributions are in the asymptotic limit to within our statistical measurement uncertainties. One issue for this measurement is whether or not the interactions are switched off sufficiently quickly to accurately measure $n(k)$. The data in Fig. 1(a) were taken using a magnetic-field sweep rate of $\dot{B} = 1.2 \frac{G}{\mu s}$ to turn off the interactions for the expansion. In the inset to Fig. 1a, we show the dependence of the measured $C$ on $\dot{B}$. Using an empirical exponential fit [line in Fig. 1(a) inset], we estimate that for our typical $\dot{B}$ of 1.2 to 1.4 $\frac{G}{\mu s}$, $C$ is systematically low by about 10%. We have therefore scaled $C$ measured with this method by 1.1.

The contact is also manifest in rf spectroscopy, where one applies a pulsed rf field and counts the number of atoms that are transferred from one of the two original spin states into a third, previously unoccupied, spin state [11]. We transfer atoms from the $|9/2, -7/2\rangle$ state to the $|9/2, -5/2\rangle$ state. It is predicted that the number of atoms transferred as a function of the rf frequency, $\nu$, scales as $\nu^{-3/2}$ for large $\nu$, and that the amplitude of this high frequency tail is $\frac{C}{2^{3/2}\pi^2}$ [12–14]. Here, $\nu = 0$ is the single-particle spin-flip resonance, and $\nu$ is given in units of $E_F/h$. This prediction requires that atoms transferred to the third spin-state have only weak interactions with the other atoms so that "final-state effects" are small [14–21], as is the case for $^{40}$K atoms. In Fig. 1(b), we plot a measured rf spectrum, $\Gamma(\nu)$, multiplied by $2^{3/2}\pi^2\nu^{3/2}$. The rf spectrum is normalized so that its integral equals 0.5. We observe the predicted $1/\nu^{3/2}$ behavior for large $\nu$, and obtain $C$ by averaging $2^{3/2}\pi^2\nu^{3/2}\Gamma(\nu)$ for $\nu > \nu_C$, where we use $\nu_C = 5$ for $(k_F a)^{-1} > -0.5$ and $\nu_C = 3$ for $(k_F a)^{-1} < -0.5$. These values for $\nu_C$ are chosen such that for $\nu \geq \nu_C$, $\Gamma(\nu)$ is in its asymptotic limit.

The connection between $\Gamma(\nu)$ and the high-$k$ tail of $n(k)$ can be seen in the Fermi spectral function, which can be probed using photoemission spectroscopy for ultra cold atoms [8]. Recent photoemission spectroscopy results on a strongly interacting Fermi gas [22] revealed a weak, negatively dispersing feature at high $k$ that persists to temperatures well above $T_F$. This feature was attributed to the effect of interactions, or the contact, consistent with a recent prediction [23]. Atom photoemission spectroscopy, which is based upon momentum-resolved rf spectroscopy, also provides a method for measuring $n(k)$. By integrating over the energy axis, or equivalently, summing data taken for different rf frequencies, we obtain $n(k)$. This alternative method for measuring $n(k)$ yields results similar to the ballistic expansion technique, but avoids the issue of magnetic-field sweep rates.

In Fig. 2, we show the measured contact for different values of $1/k_F a$. We restrict the data to values of $1/k_F a$ where our magnetic-field sweeps are adiabatic [24].

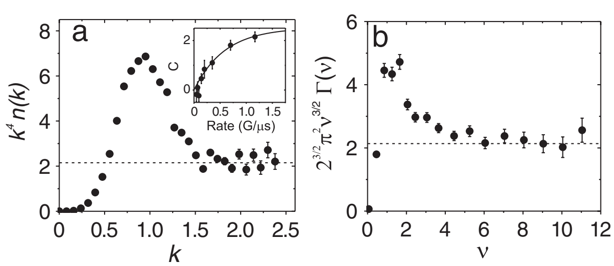


FIG. 1. *Extracting the contact from the momentum distribution and rf line shape.* (a) Measured momentum distribution for a Fermi gas at $\frac{1}{k_F a} = -0.08 \pm 0.04$. Here, the wave number $k$ is given in units of $k_F$, and we plot the normalized $n(k)$ multiplied by $k^4$. The dashed line corresponds to 2.2, which is the average of $k^4 n(k)$ for $k > 1.85$. (Inset) The measured value for $C$ depends on the rate of the magnetic-field sweep that turns off the interactions before time-of-flight expansion. (b) rf line shape measured for a Fermi gas at $\frac{1}{k_F a} = -0.03 \pm 0.04$. Here, $\nu$ is the rf detuning from the single-particle Zeeman resonance, given in units of $E_F/h$. We plot the normalized rf line shape multiplied by $2^{3/2}\pi^2\nu^{3/2}$, which is predicted to asymptote to $C$ for large $\nu$. Here, the dashed line corresponds to 2.1, from an average of the data for $\nu > 5$.

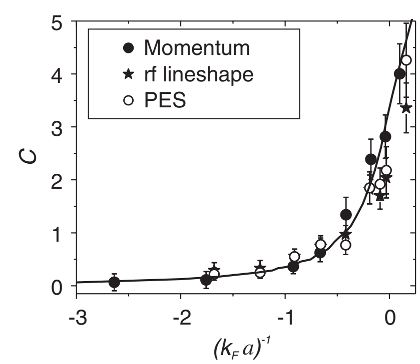


FIG. 2. *The contact.* We measure the contact, $C$, as a function of $(k_F a)^{-1}$ using three different methods. Filled circles correspond to direct measurements of the fermion momentum distribution $n(k)$ using a ballistic expansion, in which a fast magnetic-field sweep projects the many-body state onto a noninteracting state. Open circles correspond to $n(k)$ obtained using atom photoemission spectroscopy measurements. Stars correspond to the contact obtained from rf spectroscopy. The values obtained with these different methods show good agreement. The contact is nearly zero for a weakly interacting Fermi gas with attractive interactions (left hand side of plot) and then increases as the interaction strength increases to the unitarity regime where $(k_F a)^{-1} = 0$. The line is a theory curve obtained from Ref. [5].

Figure 2 shows $C$ extracted using the three different techniques described above to probe two distinct microscopic quantities, namely, $n(k)$ and $\Gamma(\nu)$. We find that the amplitude of the $1/k^4$ tail of $n(k)$ and the coefficient of the $1/\nu^{3/2}$ tail of $\Gamma(\nu)$ yield consistent values for $C$. The error bars shown in Fig. 2 include both statistical and estimated systematic uncertainties, which are roughly equal in magnitude. In extracting $C$ from the rf measurements, the largest source of systematic error comes from residual interactions with atoms in third spin state [14]. For the ballistic expansion measurements, the systematic uncertainty is dominated by the effect of the finite $\dot{B}$. For comparison with the data, the solid line in Fig. 2 shows a prediction for $C$ that was reported in Ref. [5]. This zero temperature prediction consists of the BCS limit, interpolation of Monte Carlo data near unitarity, and the BEC limit, and uses a local density approximation.

Remarkably, the Tan relations predict that the contact is also directly connected to the thermodynamics of the gas. The total energy of the trapped gas per particle, $E$, is the sum of three contributions, the kinetic energy $T$, the external potential energy $V$, and the interaction energy $I$. To test the Tan relations, we measure the potential energy, $V$, and release energy, $T + I$, of the cloud.

We measure $V$ by imaging the spatial distribution of the atom cloud [25]. We allow the cloud to expand for 1.6 ms to lower the optical density and then image along one of the radial directions. Because the expansion time is 30 times shorter than the axial trap period, the density distribution in the axial direction reflects the in-trap density distribution. The potential energy per particle, in units of $E_F$, is then $V = \frac{3}{E_F}\frac{1}{2}m\omega_z^2\langle z^2\rangle$, where $\langle z^2\rangle$ is the mean squared width of the cloud in the axial direction, and we have assumed that the potential energy is distributed equally in $x$, $y$, and $z$.

To measure $T + I$, we turn off the trap suddenly and let the cloud expand for $t = 16$ ms (with interactions) before imaging along one of the radial directions; this is similar to measurements reported in Ref. [26]. The total release energy is the sum of the release energy in the two radial directions and the release energy in the axial direction. For the radial direction, the release energy per particle, in units of $E_F$, is simply $T_r + I_r = \frac{2}{E_F}\frac{1}{2}m\frac{\langle y^2\rangle}{t^2}$ where t is the expansion time and $\langle y^2\rangle$ is the mean squared width of the expanded cloud in the radial direction. For the axial direction, the expansion is slower, and the expanded cloud may not be much larger than the in-trap density distribution. This is especially true near the Feshbach resonance where the cloud expands hydrodynamically [27]. Accounting for this, the axial release energy is $T_z + I_z = \frac{1}{E_F}\frac{1}{2}m\frac{\langle z^2\rangle - z_0^2}{t^2}$, where $z_0^2$ is the mean squared axial width of the in-trap density distribution.

We extract the mean squared cloud widths from surface fits to the images, where we fit to a finite temperature Fermi-Dirac distribution. Rather than being theoretically motivated, we simply find empirically that this functional form fits well to our images. In order to extract the energy, we perform a weighted fit where each point in the image is weighted by the square of the distance from the center of the cloud. To eliminate systematic error due to uncertainty in the trap frequencies and imaging magnification, we measure the release energy and potential energy of a very weakly interacting Fermi gas at $\frac{T}{T_F} = 0.11$, where we expect $T + I = V = 0.40E_F$. We then use the ratio of $0.40E_F$ to our measured values as a multiplicative correction factor that we apply to the data. This correction is within 5% of unity. For the point with $\frac{1}{k_F a} > 0$, we add the binding energy of the molecules, $-1/(k_F a)^2$, to the release energy, $T + I$. The energies $V$ and $T + I$ are shown versus $(k_F a)^{-1}$ in the inset of Fig. 3, where the error bars include both statistical and systematic sources of uncertainty, which are roughly equal in magnitude.

We can now test the predicted universal relations connecting the $1/k^4$ tail of the momentum distribution with the thermodynamics of the trapped Fermi gas. We first consider the adiabatic sweep theorem [1],

$$2\pi\frac{dE}{d[-1/(k_F a)]} = C, \tag{2}$$

which relates the contact $C$ to the change in the total energy of the system when the interaction strength is changed adiabatically. The inset to Fig. 3 shows $E$ obtained by summing the measured values for $T + I$ and $V$. To test the adiabatic sweep theorem, we find the derivative, $\frac{dE}{d[-1/(k_F a)]}$, simply by calculating the slope for pairs of neighboring points in the inset of Fig. 3. In the main part of Fig. 4, we compare this point-by-point derivative, multiplied by $2\pi$, to $C$ obtained from the weighted averages of the data shown in Fig. 2 ( $\circ$ ). Comparing these measurements of the left and right sides of Eq. (2), we find good agreement and thus verify the adiabatic sweep theorem for our strongly interacting Fermi gas.

A second universal relation that we can directly test is the generalized virial theorem [1],

$$E - 2V = T + I - V = -\frac{C}{4\pi k_F a}, \tag{3}$$

which is predicted to be valid for all values of the interaction strength $(k_F a)^{-1}$. This generalized virial theorem reduces to $E - 2V = 0$ for the ideal gas, where $I = 0$, as well as for the unitarity gas, where $(k_F a)^{-1} = 0$. The result for the unitarity gas was previously verified in Ref. [28]. Here, we test Eq. (3) for a range of interaction strengths. In Fig. 4, we plot the measured difference $T + I - V$ versus $(k_F a)^{-1}$ along with $\frac{C}{4\pi k_F a}$, where we use our direct measurements of $C$. We find that these independent measurements of the left and the right sides of Eq. (3) agree to within the error bars, which include both statistical and systematic sources of uncertainty. It is interesting to note that the measured energy difference $T + I - V$ is small (in units of $E_F$) so that even a Fermi gas with a strongly

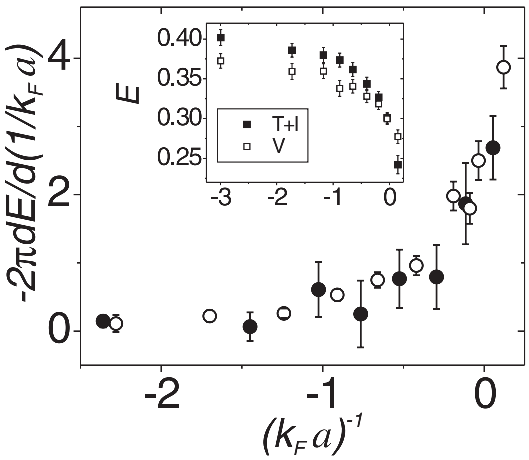


FIG. 3. *Testing the adiabatic sweep theorem.* (Inset) The measured potential energy, $V$, and release energy, $T + I$, per particle in units of $E_F$ are shown as a function of $1/k_F a$. (Main) Taking a discrete derivative of the inset data, we find that $2\pi \frac{dE}{d[-1/(k_F a)]}$ (•) agrees well with the average value of $C$ obtained from the measurements shown in Fig. 2 (∘).

attractive contact interaction nearly obeys the noninteracting virial equation.

In conclusion, we have measured the integrated contact for a strongly interacting Fermi gas and demonstrated the connection between the $1/k^4$ tail of the momentum distribution and the high frequency tail of rf spectra. Combining a measurement of $C$ vs $(k_F a)^{-1}$ with measurements of the potential energy and the release energy of the trapped gas, we verify two universal relationships [1], namely, the adiabatic sweep theorem and the generalized virial theorem. These universal relations represent a significant advance in the understanding of many-body quantum systems with strong short-range interactions. Furthermore, these relations could be exploited to develop novel experimental probes of the many-body physics of strongly interacting quantum gases.

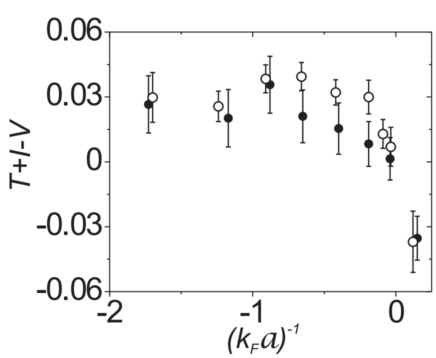


FIG. 4. *Testing the generalized virial theorem.* The difference between the measured release energy and potential energy per particle $T + I - V$ is shown as filled circles. This corresponds to the left-hand side of Eq. (3). Open circles show the right-hand side of Eq. (3) obtained from the average values of the contact shown in Fig. 2. The two quantities are equal to within the measurement uncertainty.

We acknowledge funding from the NSF and NIST. We thank A. Perali and G. C. Strinati for discussions.

*gaeblerj@jila.colorado.edu
†http://jilawww.colorado.edu/~jin/


[1] S. Tan, arXiv:abs/cond-mat/0508320v2; S. Tan, Ann. Phys. (N.Y.) **323**, 2971 (2008); S. Tan, *ibid.* **323**, 2987 (2008);S. Tan, *ibid.* **323**, 2952 (2008).
[2] E. Braaten, D. Kang, and L. Platter, Phys. Rev. Lett. **100**, 205301 (2008).
[3] L. Viverit, S. Giorgini, L. P. Pitaevskii, and S. Stringari, Phys. Rev. A **69**, 013607 (2004).
[4] S. Zhang and A. J. Leggett, Phys. Rev. A **79**, 023601 (2009).
[5] F. Werner, L. Tarruel, and Y. Castin, Eur. Phys. J. B **68**, 401 (2009).
[6] G. B. Partridge *et al.*, Phys. Rev. Lett. **95**, 020404 (2005).
[7] H. Hu *et al.*, arXiv:abs/1001.3200.
[8] J. T. Stewart, J. P. Gaebler, and D. S. Jin, Nature (London) **454**, 744 (2008).
[9] The contact is defined in the limit of $1 \ll k \ll 1/(k_F r_0)$, where $r_0$ is the range of the interatomic potential. Using a typical value of $k_F = \frac{1}{2200} a_0^{-1}$ for our trapped $^{40}$K gas and the van der Waals length, $r_0 = 60a_0$, we find $1/(k_F r_0) = 37$.
[10] C. A. Regal *et al.*, Phys. Rev. Lett. **95**, 250404 (2005).
[11] C. A. Regal, C. Ticknor, J. L. Bohn, and D. S. Jin, Nature (London) **424**, 47 (2003).
[12] P. Pieri, A. Perali, and G. C. Strinati, Nature Phys. **5**, 736 (2009).
[13] W. Schneider, V. B. Shenoy, and M. Randeria, arXiv:0903.3006v1.
[14] E. Braaten, D. Kang, and L. Platter, arXiv:1001.4518v1.
[15] C. Chin and P. S. Julienne, Phys. Rev. A **71**, 012713 (2005).
[16] Z. Yu and G. Baym, Phys. Rev. A **73**, 063601 (2006).
[17] M. Punk and W. Zwerger, Phys. Rev. Lett. **99**, 170404 (2007).
[18] S. Basu and E. J. Mueller, Phys. Rev. Lett. **101**, 060405 (2008).
[19] A. Perali, P. Pieri, and G. C. Strinati, Phys. Rev. Lett. **100**, 010402 (2008).
[20] M. Veillette *et al.*, Phys. Rev. A **78**, 033614 (2008).
[21] Y. He, C. C. Chien, Q. Chen, and K. Levin, Phys. Rev. A **77**, 011602(R) (2008).
[22] J. P. Gaebler *et al.*, arXiv:1003.1147.
[23] W. Schneider and M. Randeria, Phys. Rev. A **81**, 021601 (R) (2010).
[24] C. A. Regal, M. Greiner, and D. S. Jin, Phys. Rev. Lett. **92**, 083201 (2004).
[25] J. T. Stewart, J. P. Gaebler, C. A. Regal, and D. S. Jin, Phys. Rev. Lett. **97**, 220406 (2006).
[26] T. Bourdel *et al.*, Phys. Rev. Lett. **91**, 020402 (2003).
[27] K. M. O'Hara *et al.*, Science **298**, 2179 (2002).
[28] J. E. Thomas, J. Kinast, and A. Turlapov, Phys. Rev. Lett. **95**, 120402 (2005).